

Predictions for the synthesis of the $Z = 119$ superheavy elementJia-Xing Li (李佳星)¹ and Hong-Fei Zhang (张鸿飞)^{1,2,*}¹*School of Nuclear Science and Technology, Lanzhou University, 730000 Lanzhou, People's Republic of China*²*School of Physics, Xi'an Jiaotong University, 710049 Xi'an, People's Republic of China*

(Received 13 January 2022; accepted 9 March 2022; published 18 May 2022)

The optimal projectile-target combination and bombarding energy for the production of the new superheavy element (SHE) $Z = 119$ are predicted within the framework of a dinuclear system (DNS) model, in which the evaporation residue cross section (ERCS) is the product of capture cross section, fusion probability, and survival probability. To this end, the effects of mass asymmetry and isospin effect of target nucleus on the ERCS are analyzed. It is found that the ERCS for the production of SHE $Z = 119$ is relatively large with the ^{45}Sc projectile, while the ERCS in most cases decreases slowly with increasing neutron number of the target nucleus. We hope these predictions will shed new light timely for the recent experiments on the synthesis of the $Z = 119$ superheavy element.

DOI: [10.1103/PhysRevC.105.054606](https://doi.org/10.1103/PhysRevC.105.054606)**I. INTRODUCTION**

The synthesis of new elements $Z \geq 119$ is a frontier subject that many theorists and experimenters have devoted themselves to in recent years. To date, the synthesis of superheavy nuclei (SHN) with $Z = 110$ – 113 by using cold fusion reactions [1,2] with ^{208}Pb and ^{209}Bi targets and with $Z = 113$ – 118 by hot fusion reactions [3–5] of ^{48}Ca with actinide targets have been reported. For the synthesis of the new element $Z = 119$, not only can the eighth period of the periodic table be opened, but also a step is taken towards finding the “stable island” of SHN. It is worth noting that the ERCS used to produce SHN is very weak, limited to a few picobarns (1×10^{-12} barns). For the synthesis of the element Og ($Z = 118$), the ERCS maintains just $0.5_{-0.3}^{+1.6}$ pb [4]. These limited cross sections strongly depend on the projectile-target combination and beam energy. Therefore, theoretical research on the ERCS of superheavy element (SHE) $Z=119$ is particularly important for finding a favorable reaction and the optimal beam energy.

In recent years, many theoretical models have been proposed to study the mechanism of fusion evaporation reactions. They include the two-step model [6], the macroscopic dynamics model [7,8], multidimensional Langevin-type dynamical equations [9–14], the time-dependent Hartree-Fock theory (TDHF) [15], the extension time-dependent density-matrix theory (TDDM) [16], and the DNS model [17–26]. The above-mentioned models enable systematic investigation and comparison of production cross sections among possible combinations and predict favorable ones within each specific model. However, because different models are based on different physical images and assumptions, each model has its own advantages and disadvantages. The DNS model is one of the

models in which the nucleon transfer is coupled to the relative motion by solving a set of microscopically derived master equations (ME) that distinguish protons and neutrons [20,27]. In the DNS conception the formation of SHN is discussed as a competition between quasifission and complete fusion, and the cross sections are calculated including nuclear structure effects; these are the advantages of the DNS model. However, it is assumed that each of the two touching nuclei always keeps its own identity with its ground-state deformation [28]. Actually we know that there are nuclear and Coulomb interactions between the nuclei. Nuclei get deformed gradually due to the strong nuclear and Coulomb interactions. This deformation is not negligible, because it will alter the masses of nuclei, as well as the interactions between them, so that it will influence the further evolution of the system. The DNS conception has to be improved. The time-dependent dynamical deformation was studied numerically in Ref. [23], where the fragment deformations are coupled with nucleon transfer for heavy ion fusion reactions to form SHN. Subsequently, the evolution of fragment deformations during deeply inelastic heavy-ion collisions is considered as a dissipative process governed by the Fokker-Planck equation (FPE) under the corresponding driving potential, and analytical solutions are obtained for interaction time-dependent mean fragment quadrupole deformations in Ref. [29]. Quite recently, due to the computation restriction for solving the multivariable ME, and to further develop the DNS model, the two-variable ME (the variables of the proton and neutron number of the projectile-like fragment: Z_1, N_1) were combined with the analytical time-dependent solutions of the FPE for mean fragment deformations to treat the four variables in the process of the compound nucleus formation in Ref. [30]. The DNS model has been further developed, although there are still some shortcomings, but it has enough ability to predict the ERCS of new SHE. In this paper, within the DNS model, we systematically calculate the ERCS of isotopes with $Z = 112$ – 118 in a ^{48}Ca induced

* zhanghongfei@lzu.edu.cn

reaction and compare them with the corresponding experimental data. The results show that the ERCS calculated within the error range is consistent with the existing experimental data. This also directly illustrates the reliability of the DNS model.

Based on the reliable predictive ability of the DNS model and the urgent international desire to find favorable conditions for synthesizing new SHE $Z = 119$, we have done some work on this. We calculate several possible reactions (with stable and neutron-rich projectiles of $Z = 20\text{--}25$ and targets with half-lives longer than 20 days) leading to the formation of SHE $Z = 119$, and compare their cross sections to find the optimal projectile-target combination. Our results demonstrate that the ERCS for the production of SHE $Z = 119$ is found to be quite large with the ^{45}Sc projectile. In order to further find the best synthesis conditions, we research the influence of the target neutron number on the capture cross section, fusion probability, and survival probability for the reactions $^{45}\text{Sc} + ^{248\text{--}252}\text{Cf}$ in detail. The purpose of our research is to predict the optimal projectile-target combination and beam energy for the synthesis of SHE $Z = 119$. This article is organized as follows. In Sec. II, we introduce the DNS model. In Sec. III, numerical results are presented and discussed. Sec. IV is a brief summary.

II. THEORETICAL FRAMEWORK

Under the DNS model, the process of synthesis of SHN is divided into three steps: capture, fusion, and survival. First, two nuclei form a dual-nucleus system by overcoming the Coulomb barrier. This process is described by the capture cross section. Second, the dinuclear system fuses to a compound nucleus; in this step, there is a competition between the formation of a compound nucleus and the occurrence of quasifission. This process is described by the fusion cross section. Finally, the excited composite nucleus returns to the ground state by emitting three or four neutrons, competing with the process of fission. We use the statistical model to calculate the survival probability. In the DNS concept, the ERCS is expressed as [29,31,32]

$$\sigma_{ER}(E_{c.m.}) = \frac{\pi \hbar^2}{2\mu E_{c.m.}} \sum_J (2J+1) T(E_{c.m.}, J) \times P_{CN}(E_{c.m.}, J) \times W_{\text{sur}}(E_{c.m.}, J). \quad (1)$$

In this formula, $E_{c.m.}$ represents the center-of-mass incident energy, $T(E_{c.m.}, J)$ is the transmission probability; it means the probability that the colliding nuclei overcome the potential barrier and form a dinuclear system. $P_{CN}(E_{c.m.}, J)$ is the fusion probability. $W_{\text{sur}}(E_{c.m.}, J)$ is the survival probability of the

formed excited compound nucleus [33]. The sum is over all partial waves J .

A. Capture cross section

For the heavy ions fusion reactions, the transmission probability $T(E_{c.m.}, J)$ can be calculated by the Hill-Wheeler formula [34]:

$$T(E_{c.m.}, J) = \frac{1}{1 + \exp \left\{ -\frac{2\pi}{\hbar\omega(J)} \left[E_{c.m.} - B - \frac{\hbar^2}{2\mu R_B^2} J(J+1) \right] \right\}}. \quad (2)$$

In this formula, $\omega(J)$ represents the width at the position $R_B(J)$ of the Coulomb barrier of the parabola. Considering the quadrupole deformation, the nucleus-nucleus interaction potential can be written as [35]

$$V(r, \beta_1, \beta_2, \theta_1, \theta_2) = V_C(r, \beta_1, \beta_2, \theta_1, \theta_2) + V_N(r, \beta_1, \beta_2, \theta_1, \theta_2) + \frac{1}{2} C_1 (\beta_1 - \beta_1^0)^2 + \frac{1}{2} C_2 (\beta_2 - \beta_2^0)^2. \quad (3)$$

Here $\beta_1(\beta_2)$ is the parameter of dynamical quadrupole deformation for the projectile (target). $\beta_1^0(\beta_2^0)$ is the parameter of static deformation for the projectile (target). $\theta_1(\theta_2)$ is the angle between radius vector \vec{r} and the symmetry axes of the statically deformed projectile (target). $C_{1,2}$ are the stiffness parameters of the nuclear surface, which are calculated with the liquid drop model [36]:

$$C_i = (\lambda - 1) \left[(\lambda + 2) R_{0,i}^2 \sigma - \frac{3}{2\pi} \frac{Z_i^2 e^2}{R_{0,i} (2\lambda + 1)} \right], \quad (4)$$

where λ is the level of the dynamical deformation. Here we only consider the quadrupole deformation ($\lambda = 2$). σ is the parameter of surface tension, satisfying the relationship $4\pi R_0^2 \sigma = a_s A^{2/3}$; the parameter of surface energy $a_s = 18.32$ MeV. The expression of the Coulomb potential can be written as [37]

$$V_C(r, \beta_1, \beta_2, \theta_1, \theta_2) = \frac{Z_1 Z_2 e^2}{r} + \sqrt{\frac{9}{20\pi}} \left(\frac{Z_1 Z_2 e^2}{r^3} \right) \sum_{i=1}^2 R_i^2 \beta_i P_2(\cos \theta_i) + \left(\frac{3}{7\pi} \right) \left(\frac{Z_1 Z_2 e^2}{r^3} \right) \sum_{i=1}^2 R_i^2 [\beta_i P_2(\cos \theta_i)]^2. \quad (5)$$

The expression of the nuclear potential can be written as [38]

$$V_N(r, \beta_1, \beta_2, \theta_1, \theta_2) = -V_0 \left\{ 1 + \exp \left[\left(r - \sum_{i=1}^2 R_i (1 + (5/4\pi)^{1/2} \beta_i P_2(\cos \theta_i)) \right) / a \right] \right\}^{-1}. \quad (6)$$

Here θ_i represents the angle between the symmetry axis of the i th nucleus and the collision direction. β_i and R_i respectively

represent the quadrupole deformation parameter value of the i th nucleus and the value of the nucleus radius.

Considering the coupling channel effect through the potential barrier distribution function, the transmission probability can be written as [39]

$$T(E_{c.m.}, J) = \int f(B)T(E_{c.m.}, J)dB. \quad (7)$$

$f(B)$ is an asymmetric Gaussian distribution function:

$$f(B) = \begin{cases} \frac{1}{N} \exp \left[-\left(\frac{B-B_m}{\Delta_1} \right)^2 \right] & B < B_m, \\ \frac{1}{N} \exp \left[-\left(\frac{B-B_m}{\Delta_2} \right)^2 \right] & B > B_m. \end{cases} \quad (8)$$

Here, $B_m = \frac{B_s+B_0}{2}$, B_0 is the height of the Coulomb barrier at waist-to-waist orientation, B_s is the minimum height of the Coulomb barrier with variances of dynamical deformation β_1 and β_2 , and N is the normalization constant.

B. Complete fusion probability

In order to obtain the probability of fusion in the DNS model, we describe the fusion process as a diffusion process by numerically solving a set of master equations in the potential energy surface (PES). The time evolution of the distribution probability function [27], $P(Z_1, N_1, E_1, t)$, at time t to find Z_1 protons and N_1 neutrons in fragment 1 with excitation energy E_1 , can be described by the following master equation:

$$\begin{aligned} & \frac{dP(Z_1, N_1, E_1, t)}{dt} \\ &= \sum_{Z'_1} W_{Z_1, N_1; Z'_1, N_1}(t) \times [d_{Z_1, N_1} P(Z'_1, N_1, E_1, t) \\ & \quad - d_{Z'_1, N_1} P(Z_1, N_1, E_1, t)] \\ & \quad + \sum_{N'_1} W_{Z_1, N_1; Z_1, N'_1}(t) \times [d_{Z_1, N_1} P(Z_1, N'_1, E_1, t) \\ & \quad - d_{Z_1, N'_1} P(Z_1, N_1, E_1, t)] \\ & \quad - \{\Lambda^{qf}[\Theta(t)] + \Lambda^{fs}[\Theta(t)]\} P(Z_1, N_1, E_1, t). \end{aligned} \quad (9)$$

Here $W_{Z_1, N_1; Z'_1, N_1}$ is the mean transition probability from the channel (Z_1, N_1) to (Z'_1, N_1) , while d_{N_1, Z_1} denotes the microscopic dimension corresponding to macroscopic state (Z_1, N_1) . All the possible proton and neutron numbers of the fragment 1 are taken into the sum, but only one nucleon transfer is considered in the model ($N'_1 = N_1 \pm 1$, $Z'_1 = Z_1 \pm 1$). The evolution of the DNS along the distance between nuclei R leads to quasifission. The quasifission rate Λ^{qf} and Λ^{fs} fission rate are estimated with the one-dimensional Kramers formula.

The dissipated energy from the relative motion and the PES of DNS determine the excitation energy E_1 ; the PES is defined as

$$\begin{aligned} & U(N_1, Z_1; N_2, Z_2, R, \beta_1, \beta_2, J) \\ &= B(Z_1, N_1, \beta_1) + B(Z_2, N_2, \beta_2) \\ & \quad - [B(Z, N, \beta) + V_{rot}^{CN}(J)] + U_C(Z_1, Z_2, \beta_1, \beta_2, R) \\ & \quad + U_N(N_1, Z_1, N_2, Z_2, \beta_1, \beta_2, J). \end{aligned} \quad (10)$$

where $N = N_1 + N_2$ and $Z = Z_1 + Z_2$; β and β_i ($i = 1, 2$) are the quadrupole deformations of the composite nucleus and

the two fragments, respectively. $B(Z, N, \beta)$, $B(Z_1, N_1, \beta_1)$, $B(Z_2, N_2, \beta_2)$ are the binding energies of compound nucleus and the two deformed nuclei, respectively. U_C means Coulomb energy, U_N means nuclear interaction potential, and V_{rot}^{CN} means centrifugal energy.

Under the Coulomb barrier B , the formation probability of the compound nucleus can be expressed as

$$P_{CN}(E_{c.m.}, J, B) = \sum_{Z_1=1}^{Z_{BG}} \sum_{N_1=1}^{N_{BG}} P(Z_1, N_1, E_1, \tau_{int}). \quad (11)$$

N_{BG} and Z_{BG} are the neutron number and charge number at the Businaro-Gallone (BG) point. The interaction time τ_{int} is dependent on the incident energy $E_{c.m.}$, J , and B , which are determined using the deflection function method. The fusion probability can be written as

$$P_{CN}(E_{c.m.}, J) = \int f(B)P_{CN}(E_{c.m.}, J, B)dB. \quad (12)$$

C. Survival probability

The deexcitation process of the composite nucleus in the excited state is achieved by evaporating light particles and gamma radiation; this process competes with the fission process of the excited state nuclei. The survival probability of emitting x_n neutrons can be written as

$$W_{sur}(E_{CN}^*, x, J) = P(E_{CN}^*, x, J) \prod_{i=1}^x \left[\frac{\Gamma_n(E_i^*, J)}{\Gamma_n(E_i^*, J) + \Gamma_f(E_i^*, J)} \right]. \quad (13)$$

In the formula, $E_{CN}^* = E_{c.m.} + Q$, where E_{CN}^* represents the excitation energy of the composite nuclei. E_i^* represents the excitation energy of the i th neutron before evaporation. $\Gamma_n(E_i^*, J)$ and $\Gamma_f(E_i^*, J)$ represent the partial wave decay widths of an evaporating neutron and fission respectively [35].

III. RESULTS AND DISCUSSION

A. Verify the DNS model

In order to prove the predictive ability of the DNS model, we systematically calculate the ERCS of isotopes with $Z = 112-118$ in a ^{48}Ca -induced reaction, and compared them with the corresponding experimental data [4,40-44]. Figure 1 shows a comparison of the calculated ERCS with the experimental data in the reactions $^{48}\text{Ca} + ^{238}\text{U}$, $^{48}\text{Ca} + ^{237}\text{Np}$, $^{48}\text{Ca} + ^{242}\text{Pu}$, $^{48}\text{Ca} + ^{244}\text{Pu}$, $^{48}\text{Ca} + ^{243}\text{Am}$, $^{48}\text{Ca} + ^{245}\text{Cm}$, $^{48}\text{Ca} + ^{248}\text{Cm}$, $^{48}\text{Ca} + ^{249}\text{Bk}$, and $^{48}\text{Ca} + ^{249}\text{Cf}$. The ERCS calculated by the DNS model can describe the experimental values well within the error range. Especially for the reactions $^{48}\text{Ca} + ^{242}\text{Pu}$, $^{48}\text{Ca} + ^{244}\text{Pu}$, $^{48}\text{Ca} + ^{243}\text{Am}$, $^{48}\text{Ca} + ^{245}\text{Cm}$, these results coincide well with the experimental data.

B. Influence of the mass asymmetry on ERCS

We calculate the ERCS of the reactions that can produce the same compound nucleus in Fig. 2. Our results show that the ERCS decrease by about two orders of magnitude with increasing charge number of the projectile. This is due to the

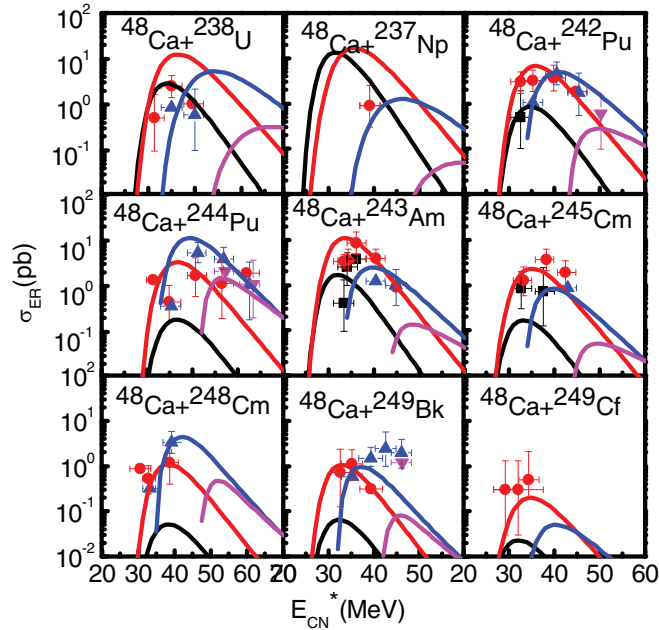


FIG. 1. Calculated ERCS compared with available experimental data. Measured ERCS of the $2n$, $3n$, $4n$, and $5n$ channels are denoted by black square, red circle, blue normal triangle, and pink inverted triangle, respectively. Calculated results are denoted by solid lines.

strong decrease in fusion probability with decreasing mass asymmetry in the entrance channel. As shown in Fig. 2, the use of a ^{51}V beam is less favorable than ^{45}Sc . This is attributable to a lower fusion probability of the $^{51}\text{V} + ^{244}\text{Cm}$ fusion reaction. Our calculations also demonstrated that the use of a ^{55}Mn beam instead of ^{45}Sc decreases the ERCS, owing to a lower fusion probability. In order to clarify the changes in the fusion probability of these reactions, we must analyze their driving potential.

In Fig. 3, it is easy to see from the physical image of the driving potential that the dinuclear system moves from the entrance channel position to the left of the BG point.

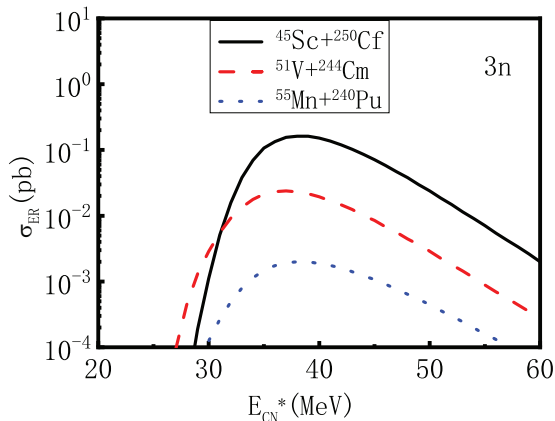


FIG. 2. Evaporation residue excitation functions in production of isotopes of superheavy nuclei $Z = 119$ in reactions $^{45}\text{Sc} + ^{250}\text{Cf}$, $^{51}\text{V} + ^{244}\text{Cm}$, and $^{55}\text{Mn} + ^{240}\text{Pu}$.

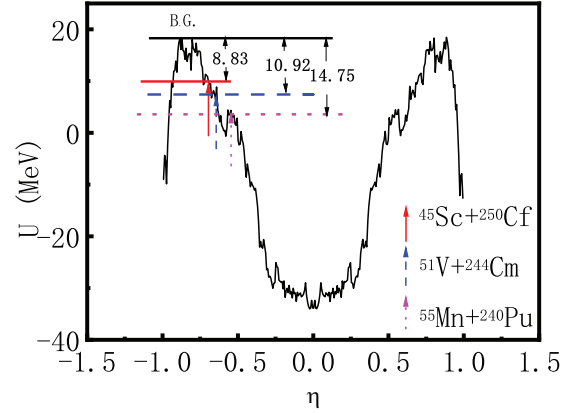


FIG. 3. The PES for the reactions $^{45}\text{Sc} + ^{250}\text{Cf}$, $^{51}\text{V} + ^{244}\text{Cm}$, and $^{55}\text{Mn} + ^{240}\text{Pu}$ as a function of mass asymmetry η . The arrow in the figure indicates the entrance channel.

In the process of evolution, there is a potential barrier B_{fus} to prevent this evolution trend. In other words, in order to trigger a fusion reaction, the dinuclear system must overcome this potential barrier, which is called the inner fusion barrier. One can see that the inner fusion barrier of the $^{45}\text{Sc} + ^{250}\text{Cf}$ reaction is smaller than that of the other two reactions, because its mass asymmetry is relatively large. That is to say, as the mass asymmetry increases, the inner fusion barrier of the dinuclear system becomes smaller, resulting in an increase in the probability of fusion. Therefore, we predict that the more suitable projectile-target combinations for synthesizing SHE $Z = 119$ are the reactions $^{45}\text{Sc} + ^A\text{Cf}$.

C. Influence of the target neutron number on ERCS

In order to further find the best synthesis conditions, it is necessary to study the isospin dependence of the ERCS on the target nucleus. The calculated maximal ERCS and the corresponding optimal excitation energies of the compound nuclei in the $3n$ evaporation channel are presented in Fig. 4 for the reactions $^{45}\text{Sc} + ^A\text{Cf}$ as functions of the mass number A of the target, respectively. Figure 4(a) shows that the Q values increase with the increase in neutron number. Figure 4(b) shows that the maximum ERCS decrease with the increase in neutron number. Figure 4(c) indicate that the excitation energies fluctuate between 38 and 40 MeV with the increase in neutron number. To analyze the trend of the change above, the whole process of SHE synthesis needs to be investigated in detail. Next, we investigate the influence of the target neutron number on the capture cross section, fusion probability, and survival probability.

Figure 5 shows that the capture cross sections σ_{cap} as a function of the excitation energy are quite close to each other for the five above-mentioned reactions owing to a slight difference in Coulomb barriers. In the lower excitation energy region $E_{CN}^* < 40$ MeV, the σ_{cap} for the reaction $^{45}\text{Sc} + ^{248}\text{Cf}$ is larger than those of $^{45}\text{Sc} + ^{249}\text{Cf}$, $^{45}\text{Sc} + ^{250}\text{Cf}$, $^{45}\text{Sc} + ^{251}\text{Cf}$, and $^{45}\text{Sc} + ^{252}\text{Cf}$ because of the large negative Q values ($E_{CN}^* = E_{c.m.} + Q$) of the former reaction. When the

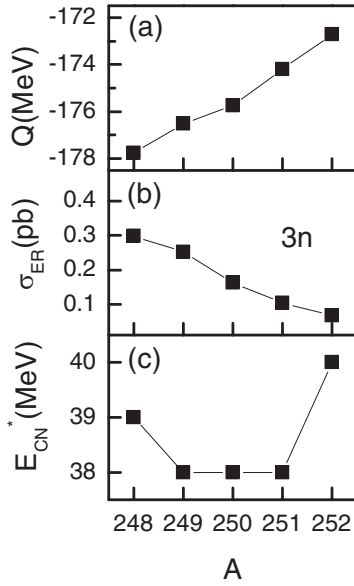


FIG. 4. Isospin dependence from $^{45}\text{Sc} + {}^A\text{Cf}$ fusion reactions: (a) Q values for fusion reactions $^{45}\text{Sc} + {}^A\text{Cf}$; (b) maximal evaporation residue cross sections as functions of target mass number A , for $3n$ emission channels; (c) corresponding excitation energies of compound nuclei.

excitation energy $E_{CN}^* \geq 40$ MeV, the σ_{cap} tend to be almost consistent.

Figure 6 shows the fusion probability P_{CN} as a function of the excitation energy of the compound nucleus for the reactions $^{45}\text{Sc} + {}^{248-252}\text{Cf}$. One can see that the fusion probability P_{CN} changes irregularly with increasing neutron number in the lower excitation energy region. However, when excitation energy increases beyond 30 MeV, the fusion probability P_{CN} decreases with increasing neutron number. P_{CN} depends on the details of the driving potential, which is decided by the properties of the nuclei in each DNS and their interactions.

Figure 7 shows the survival probability W_{sur} as a function of the excitation energy of the compound nucleus. In the lower excitation energy region $E_{CN}^* < 40$ MeV, the survival

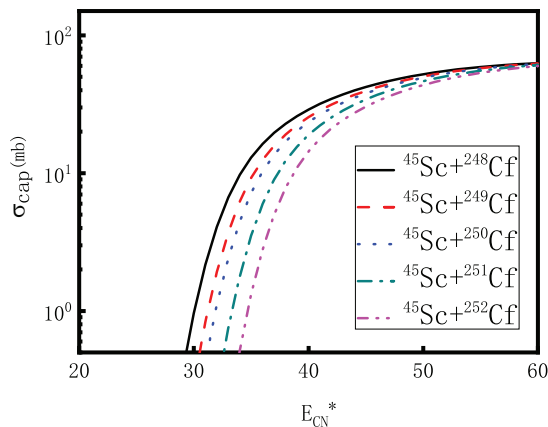


FIG. 5. Capture cross sections as functions of excitation energy of compound nuclei.

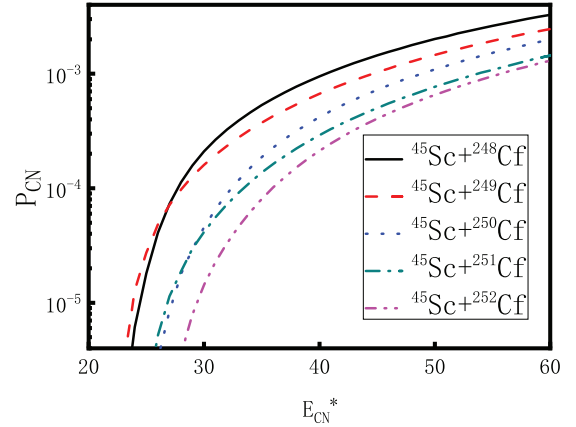


FIG. 6. Fusion probabilities as functions of excitation energy of compound nuclei.

probability W_{sur} increases with increasing neutron number. When excitation energy increases beyond 40 MeV, the differences between survival probabilities among the five reactions become very small, and the results tend to be consistent.

In summary, for the reactions $^{45}\text{Sc} + {}^{248}\text{Cf}$, $^{45}\text{Sc} + {}^{249}\text{Cf}$, $^{45}\text{Sc} + {}^{250}\text{Cf}$, $^{45}\text{Sc} + {}^{252}\text{Cf}$, and $^{45}\text{Sc} + {}^{252}\text{Cf}$, the excitation energy corresponding to their maximum ERCS is very high (about 40 MeV). Under this excitation energy, the capture cross section σ_{cap} and fusion probability P_{CN} decrease with increasing neutron number, and the survival probability W_{sur} increases with increasing neutron number. The calculated maximal ERCS σ_{3n} decreases with the increase in neutron number.

D. Production cross sections of SHE $Z = 119$

In this work, we analyzed the influence of mass symmetry and the target neutron number on the maximum ERCS. Our investigation shows that the reaction $^{45}\text{Sc} + {}^{248}\text{Cf}$ is the best candidate channel for synthesizing the new SHE $Z = 119$. In order to make the research more extensive, the maximum ERCS of some probable candidates for synthesising SHE

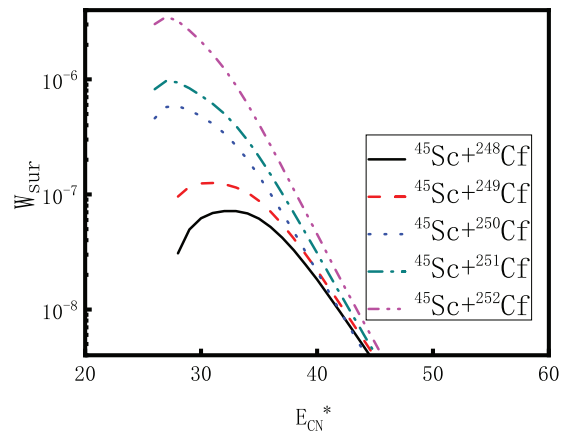


FIG. 7. Survival probabilities as functions of excitation energy of compound nuclei (in the $3n$ channel).

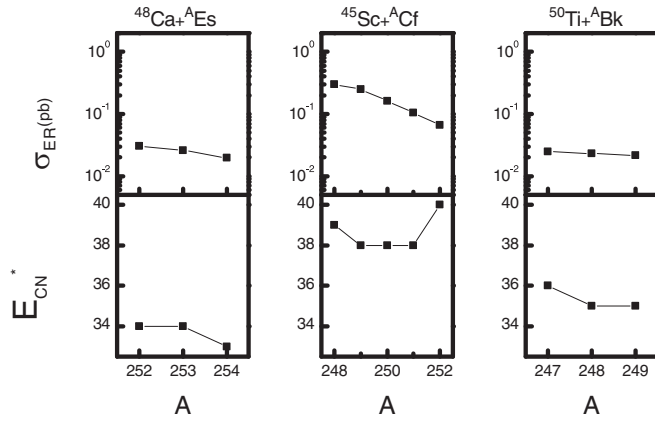


FIG. 8. Isospin dependence of maximal ERCS and excitation energies of compound nuclei corresponding to the maximal ERCS from fusion reactions: $^{48}\text{Ca} + ^A\text{Es}$, $^{45}\text{Sc} + ^A\text{Cf}$, $^{50}\text{Ti} + ^A\text{Bk}$, as functions of target mass number A , for $3n$ emission channels.

$Z = 119$ are investigated. We observed that the maximum ERCS of these reactions all appeared in the $3n$ evaporation channel. The maximum ERCS for $3n$ emission channels out of ^{48}Ca , ^{45}Sc , ^{50}Ti , ^{51}V , ^{54}Cr , and ^{55}Mn bombarding actinide isotopic chains ^AEs , ^ACf , ^ABk , ^ACm , ^AAm , and ^APu are shown in Figs. 8 and 9 as a function of the mass number of the target. Figure 8 and 9 show that the isotopes of target nuclei with smaller neutron excess are favorable for most cases of synthesizing SHE $Z = 119$. In all cases the ERCS basically decrease with increasing neutron number, though sometimes not very distinctly. Finally, for these reactions, we also investigate the influence of the target neutron number on the capture cross section, fusion probability, and survival probability. Similarly to the results of the reactions $^A\text{Sc} + ^{248}\text{Cf}$, under the excitation energy of the compound nucleus corresponding to maximal ERCS, our calculations show that, for $3n$ emission, the capture cross section σ_{cap} and fusion probability P_{CN} decrease with increasing neutron number, and the survival probability W_{sur} increases with increasing neutron number. Finally, the $3n$ evaporation channel corresponding to the ERCS decreases with the increase in the neutron number.

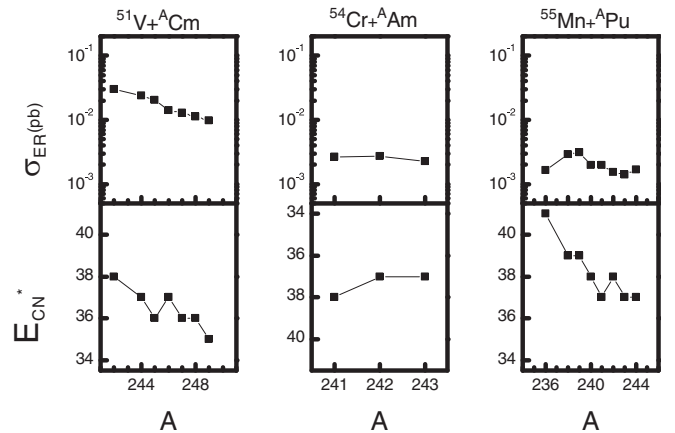


FIG. 9. Isospin dependence of maximal ERCS and excitation energies of compound nuclei corresponding to the maximal ERCS from fusion reactions: $^{51}\text{V} + ^A\text{Cm}$, $^{54}\text{Cr} + ^A\text{Am}$, $^{55}\text{Mn} + ^A\text{Pu}$, as functions of target mass number A , for $3n$ emission channels.

IV. SUMMARY

To investigate the most suitable projectile-target combination for the synthesis of SHE $Z = 119$, the projectiles ^{48}Ca , ^{45}Sc , ^{50}Ti , ^{51}V , ^{54}Cr , and ^{55}Mn bombarding some actinide isotopic chains are systematically studied within the DNS model. Our results demonstrate that the strong dependence of the calculated ERCS on mass asymmetry in the entrance channel makes the ^{45}Sc projectile the most promising for further synthesis of SHE $Z = 119$. The influence of the target neutron number on ERCS is also investigated. Our results demonstrate that, under the excitation energy of the compound nucleus corresponding to maximal ERCS, the P_{CN} change with increasing neutron number of the target is relatively significant. Thus, the $3n$ evaporation channel corresponding to the ERCS basically decreases with the increase in the neutron number owing to the P_{CN} decreasing with increasing neutron number. Finally, we predict that for the synthesis of the SHE $Z = 119$ the maximal ERCS is 0.29 pb, reached by the reaction $^{45}\text{Sc} + ^{248}\text{Cf}$ with an incident energy of 216.77 MeV. Hopefully, the theoretical prediction results will shed light on the experimental synthesis of this new element.

[1] S. Hofmann and G. Münzenberg, *Rev. Mod. Phys.* **72**, 733 (2000).
 [2] K. Morita, K. Morimoto, D. Kaji, H. Haba, K. Ozeki, Y. Kudou, T. Sumita, Y. Wakabayashi, A. Yoneda, K. Tanaka, S. Yamaki, R. Sakai, T. Akiyama, S.-i. Goto, H. Hasebe, M. Huang, T. Huang, E. Ideguchi, Y. Kasamatsu, K. Katori *et al.*, *J. Phys. Soc. Jpn.* **81**, 103201 (2012).
 [3] Y. T. Oganessian, F. S. Abdullin, P. D. Bailey, D. E. Benker, M. E. Bennett, S. N. Dmitriev, J. G. Ezold, J. H. Hamilton, R. A. Henderson, M. G. Itkis, Y. V. Lobanov, A. N. Mezentsev, K. J. Moody, S. L. Nelson, A. N. Polyakov, C. E. Porter, A. V. Ramayya, F. D. Riley, J. B. Roberto, M. A. Ryabinkin *et al.*, *Phys. Rev. Lett.* **104**, 142502 (2010).

[4] Y. T. Oganessian, V. K. Utyonkov, Y. V. Lobanov, F. S. Abdullin, A. N. Polyakov, R. N. Sagaidak, I. V. Shirokovsky, Y. S. Tsyganov, A. A. Voinov, G. G. Gulbekian, S. L. Bogomolov, B. N. Gikal, A. N. Mezentsev, S. Iliev, V. G. Subbotin, A. M. Sukhov, K. Subotic, V. I. Zagrebaev, G. K. Vostokin, M. G. Itkis *et al.*, *Phys. Rev. C* **74**, 044602 (2006).
 [5] Y. Oganessian, *J. Phys. G: Nucl. Part. Phys.* **34**, R165 (2007).
 [6] C. Shen, Y. Abe, D. Boilley, G. Kosenko, and E. Zhao, *Int. J. Mod. Phys. E* **17**, 66 (2008).
 [7] S. Bjornholm and W. Swiatecki, *Nucl. Phys. A* **391**, 471 (1982).
 [8] W. Swiatecki, *Prog. Part. Nucl. Phys.* **4**, 383 (1980).
 [9] V. Zagrebaev and W. Greiner, *Nucl. Phys. A* **944**, 257 (2015), Special Issue on Superheavy Elements.
 [10] V. I. Zagrebaev, *Phys. Rev. C* **64**, 034606 (2001).

- [11] V. Zagrebaev and W. Greiner, *J. Phys. G: Nucl. Part. Phys.* **34**, 1 (2006).
- [12] V. Zagrebaev and W. Greiner, *Phys. Rev. C* **78**, 034610 (2008).
- [13] V. L. Litnevsky, G. I. Kosenko, and F. A. Ivanyuk, *Phys. Rev. C* **93**, 064606 (2016).
- [14] V. L. Litnevsky, V. V. Pashkevich, G. I. Kosenko, and F. A. Ivanyuk, *Phys. Rev. C* **89**, 034626 (2014).
- [15] A. S. Umar, V. E. Oberacker, J. A. Maruhn, and P.-G. Reinhard, *Phys. Rev. C* **81**, 064607 (2010).
- [16] M. Tohyama and A. S. Umar, *Phys. Rev. C* **93**, 034607 (2016).
- [17] G. G. Adamian, N. V. Antonenko, and W. Scheid, *Phys. Rev. C* **69**, 044601 (2004).
- [18] Z.-Q. Feng, G.-M. Jin, J.-Q. Li, and W. Scheid, *Phys. Rev. C* **76**, 044606 (2007).
- [19] N. Wang, J.-q. Li, and E.-g. Zhao, *Phys. Rev. C* **78**, 054607 (2008).
- [20] Z.-Q. Feng, G.-M. Jin, and J.-Q. Li, *Phys. Rev. C* **80**, 057601 (2009).
- [21] Z.-Q. Feng, G.-M. Jin, and J.-Q. Li, *Phys. Rev. C* **80**, 067601 (2009).
- [22] M. Huang, Z. Gan, X. Zhou, J. Li, and W. Scheid, *Phys. Rev. C* **82**, 044614 (2010).
- [23] M. Huang, Z. Zhang, Z. Gan, X. Zhou, J. Li, and W. Scheid, *Phys. Rev. C* **84**, 064619 (2011).
- [24] N. Wang, E.-G. Zhao, W. Scheid, and S.-G. Zhou, *Phys. Rev. C* **85**, 041601(R) (2012).
- [25] L. Zhu, Z.-Q. Feng, C. Li, and F.-S. Zhang, *Phys. Rev. C* **90**, 014612 (2014).
- [26] S. A. Kalandarov, G. G. Adamian, N. V. Antonenko, and J. P. Wieleczko, *Phys. Rev. C* **90**, 024609 (2014).
- [27] H. Ming-Hui, G. Zai-Guo, F. Zhao-Qing, Z. Xiao-Hong, and L. Jun-Qing, *Chin. Phys. Lett.* **25**, 1243 (2008).
- [28] G. Adamian, N. Antonenko, W. Scheid, and V. Volkov, *Nucl. Phys. A* **627**, 361 (1997).
- [29] N. Antonenko, E. Cherepanov, A. Nasirov, V. Permjakov, and V. Volkov, *Phys. Lett. B* **319**, 425 (1993).
- [30] X. J. Bao, Y. Gao, J. Q. Li, and H. F. Zhang, *Phys. Rev. C* **91**, 011603(R) (2015).
- [31] W. Li, N. Wang, F. Jia, H. Xu, W. Zuo, Q. Li, E. Zhao, J. Li, and W. Scheid, *J. Phys. G: Nucl. Part. Phys.* **32**, 1143 (2006).
- [32] N. V. Antonenko, E. A. Cherepanov, A. K. Nasirov, V. P. Permjakov, and V. V. Volkov, *Phys. Rev. C* **51**, 2635 (1995).
- [33] A. S. Zubov, G. G. Adamian, N. V. Antonenko, S. P. Ivanova, and W. Scheid, *Phys. Rev. C* **65**, 024308 (2002).
- [34] D. L. Hill and J. A. Wheeler, *Phys. Rev.* **89**, 1102 (1953).
- [35] Z.-Q. Feng, G.-M. Jin, F. Fu, and J.-Q. Li, *Nucl. Phys. A* **771**, 50 (2006).
- [36] W. D. Myers and W. J. Swiatecki, *Nucl. Phys.* **81**, 1 (1966).
- [37] C. Y. Wong, *Phys. Rev. Lett.* **31**, 766 (1973).
- [38] I. I. Gontchar, D. J. Hinde, M. Dasgupta, and J. O. Newton, *Phys. Rev. C* **69**, 024610 (2004).
- [39] B. Wang, K. Wen, W.-J. Zhao, E.-G. Zhao, and S.-G. Zhou, *At. Data Nucl. Data Tables* **114**, 281 (2017).
- [40] Y. T. Oganessian, V. K. Utyonkov, Y. V. Lobanov, F. S. Abdullin, A. N. Polyakov, I. V. Shirokovsky, Y. S. Tsyganov, G. G. Gulbekian, S. L. Bogomolov, B. N. Gikal, A. N. Mezentsev, S. Iliev, V. G. Subbotin, A. M. Sukhov, A. A. Voinov, G. V. Buklanov, K. Subotic, V. I. Zagrebaev, M. G. Itkis, J. B. Patin *et al.*, *Phys. Rev. C* **70**, 064609 (2004).
- [41] Y.T. Oganessian, V.K. Utyonkov, Y.V. Lobanov, F.S. Abdullin, A.N. Polyakov, R.N. Sagaidak, I.V. Shirokovsky, Y.S. Tsyganov, A.A. Voinov, G. G. Gulbekian, S.L. Bogomolov, B. N. Gikal, A. N. Mezentsev, V.G. Subbotin, A. M. Sukhov, K. Subotic, V.I. Zagrebaev, G. K. Vostokin, M. G. Itkis, R.A. Henderson *et al.*, *Phys. Rev. C* **76**, 011601(R) (2007).
- [42] Y.T. Oganessian, V.K. Utyonkov, Y.V. Lobanov, F.S. Abdullin, A.N. Polyakov, I.V. Shirokovsky, Y.S. Tsyganov, G.G. Gulbekian, S.L. Bogomolov, B.N. Gikal, A.N. Mezentsev, S. Iliev, V.G. Subbotin, A.M. Sukhov, A.A. Voinov, G.V. Buklanov, K. Subotic, V.I. Zagrebaev, M.G. Itkis, J.B. Patin *et al.*, *Phys. Rev. C* **69**, 054607 (2004).
- [43] Y. T. Oganessian, F. S. Abdullin, S. N. Dmitriev, J. M. Gostic, J. H. Hamilton, R. A. Henderson, M. G. Itkis, K. J. Moody, A. N. Polyakov, A. V. Ramayya, J. B. Roberto, K. P. Rykaczewski, R. N. Sagaidak, D. A. Shaughnessy, I. V. Shirokovsky, M. A. Stoyer, N. J. Stoyer, V. G. Subbotin, A. M. Sukhov, Y. S. Tsyganov *et al.*, *Phys. Rev. C* **87**, 014302 (2013).
- [44] Y. T. Oganessian, F. S. Abdullin, C. Alexander, J. Binder, R. A. Boll, S. N. Dmitriev, J. Ezold, K. Felker, J. M. Gostic, R. K. Grzywacz, J. H. Hamilton, R. A. Henderson, M. G. Itkis, K. Miernik, D. Miller, K. J. Moody, A. N. Polyakov, A. V. Ramayya, J. B. Roberto, M. A. Ryabinkin *et al.*, *Phys. Rev. C* **87**, 054621 (2013).